ISSN : 0974 - 7524 Volume 6 Issue 3

Physical CHEMISTRY
An Indian Journal

Trade Science Inc.

Review

PCAIJ, 6(3), 2011 [146-162]

Surface phenomena and wetting of porous solids

R.Gajdošíková, B.Lapčíková, L.Lapčík Jr.*
Centre of Polymer Systems, Faculty of Technology, Tomas Bata University in Zlin,
nám. T.G. Masaryka 5555, 760 05 Zlín, (CZECH REPUBLIC)
E-mail: lapcik@ft.utb.cz; lapcikova@ft.utb.cz
Received: 9th May, 2011 ; Accepted: 9th June, 2011

ABSTRACT

Basic theories relating wetting phenomenon on non-ideal surface and porous solids are briefly comprised. The text comprehends thermodynamic principles of wetting, description of contact angle on ideal and non-ideal surface and capillary action with a slight remark to liquid wicking into the irregular pore structures. Further the methods used for contact angle measurement on discrete solids are mentioned which is followed by a concise review of models used for the estimation of surface free energy of solids. © 2011 Trade Science Inc. - INDIA

INTRODUCTION

The properties of surfaces and interfaces characterized by surface or interfacial tension and surface free energy are of a growing importance in recent years. These properties are joined with many phenomena concerning adhesion, wetting, spreading and wicking which express themselves in everyone's daily life, natural processes as well as in huge amount of industrial applications such as coating, printing, lubrication, composite or mineral processing, textile and wood finishing, oil recovery, painting, highly absorbent materials and adhesives[1-8]. These processes involve various materials for instance wood, paper, stone, soils, cereals and textile[9-15] which could cover all possible types of surfaces: polar, non-polar, much more often rough than smooth or even porous and this may bring many obstructions to their surface characterization.

Whilst the measurement of liquid surface tension is quite easy due to its deformability, the lack of mobility of the molecules in a solid surface precludes its direct measurement. Several independent approaches have been used to estimate solid surface energy including contact angle measurement, direct force measurement, the Lifshitz theory of van der Waals forces, the theory of molecular interactions and many others. Among these methods, contact angle measurement of pure liquids with known surface tension on a given solid surface is believed to be the simplest and the most straightforward approach. Despite the concept simplicity, practice has shown that the acquisition of thermodynamically significant contact angles requires intensive effort[1]. The value of obtained contact angle can be affected by the quality of solid surface, purity of measuring liquid, methodology etc.

There are several well-known techniques of contact angle measurement on flat and smooth surface e.g. sessile drop or adhering gas bubble method and Wilhelmy method[1,16]. Nevertheless, most of the real surfaces are not ideal but rough and heterogeneous and many materials are available only in the form of powders and fibres. It may be possible to compress these particles to obtain flat surface but such system could provide different contact angle values because

the material undergoes structural and possibly also significant chemical changes. Therefore, it would be more suitable to measure contact angles directly on the original surface.

Despite the difficulties, there are several methods which are applicable to powder and fibrous materials. The most popular is capillary rise method[1,17] and thin-layer wicking[1,18,19]. Some authors also published for instance the use of Wilhelmy method[20-22]. Furthermore, the measurements seem to yield also an additional notion of pore size and structure of the material[14,23,24], although it does not provide so extensive information such as mercury porosimetry.

The paper is intended to yield a summary of present theories and approaches used for surface properties characterization of solids.

THERMODYNAMICS OF WETTING

Surface and interfacial tension, surface free energy

The existence of surface tension of liquids causes many striking phenomena such as liquid surface bulging above a rim of a vessel, floating of pins or water drops rolling down plant leaves. There is contractile force acting on the liquid surface. It arises from the fact that molecules in the bulk of liquid phase are completely surrounded with other molecules with the intermolecular interaction radiating to all directions. The interactions may not be equivalent but outwardly they result in zero force acting on the molecules. The situation changes on the surface where the concentration of the liquid molecules is significantly lower in some directions, hence some interaction are missing and the bulk molecules tend to pull the surface molecules inward.

The contractile force is called surface tension γ and can be defined as a force acting perpendicularly to a line of unit length (l) which lies in the plain of the surface of a liquid.

The work dW done in extending a movable side by a distance dx can be expressed as:

$$dW = \gamma.l.dx \quad (1)$$

Since $l.dx = dA$ expresses the change in area, the equation (1) can be rewritten as:

$$dW = \gamma.dA = dG \quad (2)$$

Now γ represents the work done by any reversible process to form a unit area of new surface or interface. If the process is done at constant temperature T and pressure p, the increment of work will equal the increment of Gibbs free energy dG, which is also equivalent to increment of Helmholtz free energy dF under the conditions of constant temperature T and volume V, both with respect to surface area change:

$$\gamma = \left(\frac{\partial G}{\partial A}\right)_{T,p,n} = \left(\frac{\partial F}{\partial A}\right)_{T,V,n} \quad (3)$$

The letter n denotes molar amount which expresses the assumption of adsorption equilibrium[11,16,25].

Albeit the existence of the contractile force is noticeable mainly on liquid surface due to mobility of the molecules, it operates on all types of interfaces as are liquid-vapour (LV), solid-vapour (SV), solid-liquid (SL), non-miscible liquids (LL) or solids (SS). Phase boundaries including vapour phase are commonly called surfaces (liquid and solid surfaces) and the rest is named interface. When characterizing the interface properties, surface tension term is generally used for liquid surfaces, the notion of surface free energy is used for solid surfaces and the rest is designated as interfacial tension. Surface tension of liquids and interfacial tension are usually reported in mN/m whereas surface free energy is more often given in mJ/m^2. While the units are equivalent, the values of surface tension and surface free energy are equal only in the case of pure substances. For multi-component systems the surface energy can be influenced with for example temperature or volume changes accompanying mixing.

When dealing with energetics of phase boundaries, the term 'interface' is generally used, which describes the plane of the contact between two different materials. The word 'interphase' can seem to be the same but there is a significant difference especially when considering the problematic of adhesive joint and surface treatment processes. Interphase region denotes the area between the adhesive and adherent and its nature is critical for determining the properties and quality of the adhesive bond. The area of interphase has different chemical and physical characteristics than either the bulk adhesive or the adherent and may include several interfaces[26].

It should be remarked that solid surfaces very often consist of several regions without clearly defined

Review

boundaries between them. For instance polymer surface can comprise oxidation products, plasticizers, processing aids, adsorbed water, contaminants, dust etc. This often causes great variation in the surface which may affect for example joint performance without having a significant influence on the bulk properties of the material. In addition, the surfaces are dynamic systems and their nature can change rapidly immediately after preparation in response to its surroundings. Therefore it is difficult to be confident about the surface characteristic of solids[26,27].

Work of cohesion, work of adhesion and spreading

Surface tension of a liquid (as well as surface energy of a solid) is a measure of cohesion between the molecules of the same type 1. Cohesion is expressed as work of cohesion W_C (W_{11}):

$$W_C = W_{11} = 2\gamma_1 \quad (4)$$

Here γ_1 stands for the surface tension (energy) of the phase 1. It is a work required to separate a column of one phase with unit profile area whereby two new surfaces between the phase and vacuum are created.

Analogously the work of adhesion W_A is a measure of attraction forces between dissimilar molecules of two phases 1 and 2. This is stated in Dupré's equation:

$$W_A = W_{12} = \gamma_1 + \gamma_2 - \gamma_{12} \quad (5)$$

which gives a work required to separate phases 1 and 2 along the interface with unit area and to form two new surfaces of phase 1 and 2 in vacuum. It should be stated that work of cohesion and adhesion are more or less hypothetic terms because real systems are not in vacuum but other (mostly vapour) phase is present.

Now a three phase system will be under consideration where solid (S) stands for phase 1, liquid (L) for phase 2 and this is surrounded by vapour (V) phase. When the adhesion between solid and liquid molecules W_A is stronger than cohesion between liquid molecules W_C spreading occurs, which can be characterized with spreading coefficient S:

$$S = W_A - W_C = \gamma_{SV} - \gamma_{LV} - \gamma_{SL} \quad (6)$$

The relationship reveals that spreading is accompanied by the reduction of SV interface and expansion of SL and LV interface. The spreading coefficient S is positive for spontaneous process, where wetting occurs, whereas negative value of S results in a finite contact angle[11,16,28]. Perfect wetting occurs when the solid surface energy and liquid surface tension are equivalent and this observation can be used for surface characterization.

CONTACT ANGLE ON IDEAL AND NON-IDEAL SURFACE

Young equation, young-dupré equation and contact angle

Contact angle (CA) is a result of the balance of three vectors acting on the three-phase line amongst solid, liquid and vapour, namely solid surface energy γ_S (or γ_{SV}), liquid surface tension γ_L (or γ_{LV}) and solid-liquid interfacial tension γ_{SL} (Figure 1). The equilibrium was first described by Thomas Young in 1805 and thus is well known as Young equation:

$$\gamma_L \cos\theta_Y = \gamma_S - \gamma_{SL} \quad (7)$$

where θ_Y stands for Young (ideal) CA. The equation is valid even in the presence of gravitation because the gravity effect is vanishingly small in the region close to the contact line where the contact angle is given. Nevertheless, it should be stated that Young equation is defined for ideal solid surface which should be perfectly smooth, rigid, chemically homogeneous, insoluble and non-reactive[1,11,29,30].

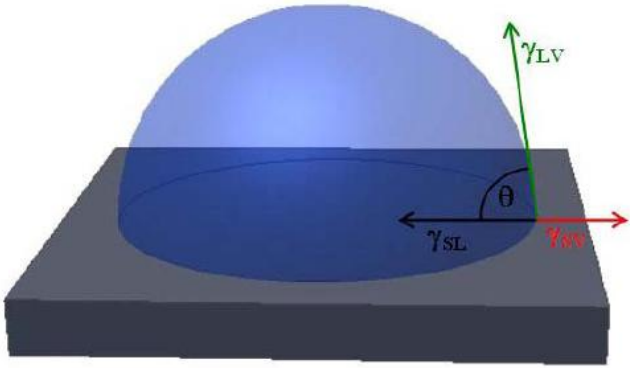

Figure 1 : Liquid drop on a solid surface

By expressing the equation (5) in terms of the solid, liquid and vapour phases as $W_A = \gamma_S + \gamma_L - \gamma_{SL}$ and introducing this into Young equation (7) following relation is obtained:

$$W_A = \gamma_L (1 + \cos\theta) \quad (8)$$

This is designated as Young-Dupré equation which creates the basis of the theory of adhesion. It enables to

formulate the correlation between the work of adhesion and the contact angle and exclude the term of SL interfacial tension γ_{SL}, which could be difficult to determine[11,31].

The value of the contact angle can range within the limits of 0° and 180°. The 0° contact angle represents the complete wetting regime in which a liquid spreads on a solid surface forming thin liquid film. In the partial wetting regime a finite contact angle is established. Surfaces with $\theta < 90°$ are usually regarded as wettable and those with $\theta > 90°$ as non-wettable. Surfaces with the drop tending to form a perfect sphere which has the 180° CA are perfectly non-wettable.

Modification of young equation

As was already mentioned, the Young equation was defined for the equilibrium on an ideal surface. Nevertheless, some modifications are believed to be requisite not only for a real surface but also for the ideal one.

In practice the solid surface energy may be lowered due to adsorption of mainly liquid but also other molecules present in the vapour phase; therefore it is necessary to take into account the conditions of each measurement. There are two possible extremes. The first is so-called 'dry' wetting which means that the solid surface is in the equilibrium only with its own vapour and the solid surface energy (SSE) remains unchanged. The second extreme is 'moist' wetting when a film of liquid molecules is adsorbed at the solid surface. The difference between SSE of 'dry' surface γ_S^0 and SSE of 'moist' surface γ_S is denoted as film pressure π_e:

$$\pi_e = \gamma_S^0 - \gamma_S \quad (9)$$

Since the adsorption process is spontaneous, the γ_S^0 value is always higher than the value of γ_S. The film pressure parameter can be introduced into Young equation:

$$\gamma_L . \cos\theta = \gamma_S^0 - \gamma_{SL} - \pi_e \quad (10)$$

The π_e parameter can be determined for example by measuring of the adsorption of liquid vapour on the solid surface in dependence on its partial pressure. However, it is generally assumed to be negligibly small especially for low-energy surfaces when a finite CA is formed and not very volatile liquids[11,28-32].

Another possible modification can be used to restrict the effect of the line tension which stems from the fact that three interfacial tensions may be influenced by each other at the contact line. Especially, the molecules of the solid could interfere with the interaction between the liquid and the vapour phase. The following equation shows the Young equation including the line tension:

$$\frac{\sigma}{R} + \gamma_L \cos\theta = \gamma_S - \gamma_{SL} \quad (11)$$

where σ is the line tension and R is the radius of the SL contact circle in the plane of the solid. Nevertheless, it may affect CA only when the drop is extremely small. For sufficiently large drops (where $R \to \infty$) the line tension is reduced to classic Young relation. Thus for practical purposes it is negligible[1,11,29].

Contact angle on rough and chemically heterogeneous surface

Solid surfaces can be rarely considered to be ideal. Mostly they are to some extend rough and chemically heterogeneous and thus obtaining Young contact angle on such surfaces is quite questionable. When speaking about non-ideal surfaces, it is necessary to distinguish actual CA and apparent CA. Actual contact angle (ACCA) is the CA between the tangent to the liquid-vapour interface and the actual (local) solid surface; whereas apparent contact angle (APCA) is the CA between the tangent to the liquid-vapour interface and the line representing the nominal solid surface, as depicted in Figure 2.

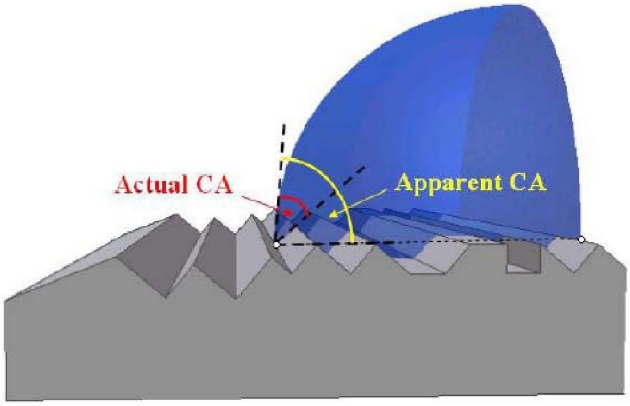

Figure 2 : Actual and apparent contact angles on rough solid surface

Actual CA is the one required but it is rarely accessible on rough surface and can be very variable on smooth but heterogeneous surface[11,29,33,34]. Since the APCA is mostly attainable, some correlations between APCA and ideal CA for various types of surfaces were

Review

discussed, but this was so far not successful[29].

Basic relationship between Young CA θ_Y and APCA on rough surface θ_W was developed by Wenzel in 1936:

$$\cos \theta_W = r \cos \theta_Y \quad (12)$$

Symbol r stands for 'roughness factor'. This factor is measurable and given as ratio of the actual versus geometric surface. For smooth surface is r = 1 but for rough surface it is always higher (r > 1) because greater amount of actual surface is wetted. The effect of roughened surface magnifies the wetting properties if either is to be more wettable or more repellent. Differences due to various degrees of roughness can be much greater than any differences caused by the nature of the materials. Therefore some substances with smooth surface and poor repelling properties can be excellently repelling in the form of fibers because of much larger amount of surface area[35]. It should be highlighted that Wenzel equation (12) is valid only in the case of 'homogeneous' wetting regime when the liquid penetrates to all the roughnesses and grooves of the surface[27,36,37].

The starting point for CA on smooth but heterogeneous surface θ_C is the Cassie equation. Concerning a surface with areas of two different chemistries 1 and 2, following equation is obtained[38]:

$$\cos \theta_C = f_1 \cos \theta_1 + f_2 \cos \theta_2 \quad (13)$$

f_1 and f_2 denote fraction of area containing component 1 and 2 ($f_1+f_2=1$) and θ_1 and θ_2 are respective CA of components 1 and 2. This can be generalized for surface which comprises i-chemistries with i-contact angles, as can be seen in following equation[27,39]:

$$\cos \theta_C = \Sigma f_i \cos \theta_i \quad (14)$$

When the surface roughness is too high, air bubbles may be trapped in the grooves under the liquid. This is so called 'heterogeneous' or 'air-pocket' wetting regime[29,36,37]. Such surface can be regarded as composite consisting of two components with different wettability – air and solid material. In this case Cassie equation can be modified as:

$$\cos \theta_{CB} = fr_f \cos \theta_Y - (1 - f) \quad (15)$$

This relation was developed by Cassie and Baxter[40]. The meaning of the symbols is subsequent: f is fraction of projected area wetted by liquid and r_f is the roughness ratio of the wet area.

The transition between homogeneous and heterogeneous regime depends on the geometry of surface[29]. Heterogeneous wetting is very important mainly for ultra-hydrophobic applications based on so called 'lotus effect' and self-cleaning applications[37,41,42].

Advancing and receding contact angles and hysteresis

Contact angle interpretation can be escorted by many difficulties because a wide range of practically stable CAs may appear on a real surface. When the volume of a drop is increased during an experiment, the three phase contact line is pinned but remains fixed and the CA grows until the maximum value is reached, which is referred as 'advancing' CA Θ_A. After that the advancing of the contact line occurs, whereas a new dry area is wetted, which is sometimes called a 'stick-slip' mode. Analogically, if the drop volume is increased, CA diminishes until its minimum value, called 'receding' CA Θ_R, and then the contact line recedes[29,43]. The same arises for example during a solid is pushed in or pulled out of a liquid, capillary elevation and depression or inclination of the solid surface.

The difference between advancing and receding CA is hysteresis H which is zero for ideal surface and rises as the surface deviates from ideality. To some extend the hysteresis can be used to examine the non-ideality of surface. Three major causes of the hysteresis have been invoked which are surface roughness, chemical contaminations in the solid surface and solutes in the liquid which may deposit on the solid surface[43]. It was suggested using the advancing and receding CA to obtain the most stable APCA θ_{MS} on non-ideal surface, which can be estimated by relation:

$$\theta_{MS} = (\theta_A + \theta_R) / 2 \quad (16)$$

It can be also expressed as arithmetic mean of CA cosines. This is denoted as hysteresis approach but so far it was not sufficiently substantiated[3,29].

It should be stated that when the CA lies within the interval $[\theta_A; \theta_R]$ the contact line remains more or less immobile but as the three-phase line begins to move, the CA becomes to be dynamic and changes along with the velocity of contact line[3,44]. This 'dynamic' CA θ_D and can significantly vary from the CA gained under static condition θ_S, which is very important for most practical applications because overwhelming majority of manufacturing processes are dynamic.

CAPILLARITY, WETTING OF POROUS SOLIDS

A very large class of the artificial and natural processes involves porous bodies that are wetted by liquids such as printing on paper, coating of wood, water percolation in soil. Liquid penetration in porous solids is in general governed partly by the surface energy represented by the contact angle and partly by capillarity which depends on the geometry of the system.

Laplace equation

In the case of partial wetting the surface forces tend to make liquid-vapour interface spherical. There is a pressure difference ΔP operating across the curved interface. The pressure is greater at the concave side and the pressure drop is proportional to the radius of curvature and the surface tension of the liquid. This relation of pressure difference and the curvature of the surface describes Young-Laplace equation of capillarity, which was derived in 1805:

$$\Delta P = \gamma_L \left(\frac{1}{R_1} + \frac{1}{R_2} \right) \quad (17)$$

where R_1 and R_2 denote the principal radii of curvature of the interface. For hemispherical LV interface which has only one radius of curvature ($R_1 = R_2 = R$), the Young-Laplace equation acquires following form:

$$\Delta P = \frac{2\gamma_L}{R} \quad (18)$$

In the case of the planar surface is the pressure difference equal to zero[13,30,45].

Lucas-Washburn equation

Wetting of porous solids is caused by capillary penetration. The simplest theoretical model used to describe this situation is a liquid penetration into a cylindrical capillary filled with vapour phase (with negligible density) which is dipped in the sufficiently large liquid reservoir so as the meniscus shape of the liquid in capillary is not influenced by the liquid meniscus curvature in reservoir, as shown in Figure 3. Flow of the liquid is driven by the pressure difference across the LV interface as given by Young-Laplace equation (17).

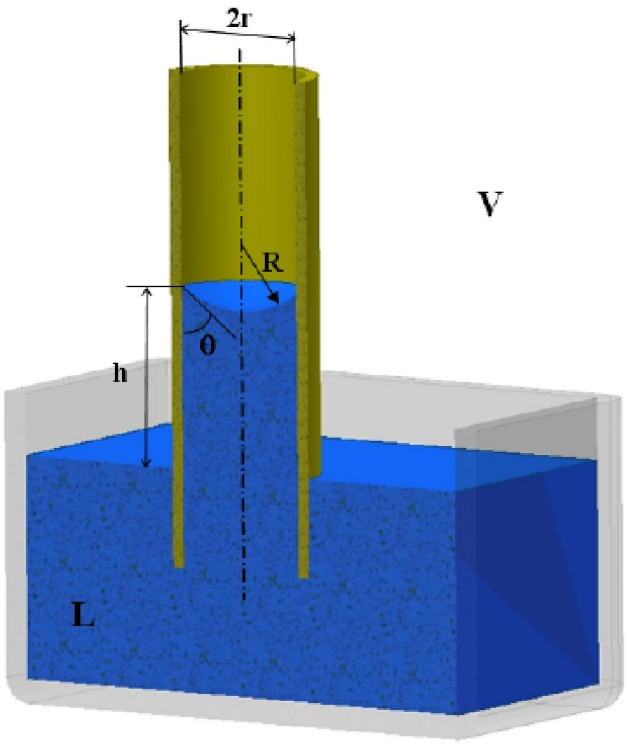

Figure 3 : Liquid penetration into a cylindrical capillary

If the capillary is cylindrical and its walls are perfectly wettable by the penetrating liquid, then the meniscus is assumed to be perfectly hemispherical (the interface radius of curvature R equals to internal capillary radius r) and the pressure difference across the LV interface is given by eq. (18). If there is a certain apparent CA between the capillary wall and LV interface and spherical meniscus then $R_1 = R_2 = r/\cos\theta$ and the pressure difference is given by the relation:

$$\Delta P = \frac{2\gamma_L \cos\theta}{r} \quad (19)$$

It should be emphasized that the apparent CA is the one which influence this system.

The pressure difference is the driving force of capillary penetration which is balanced by viscous dissipation of the liquid, the hydrostatic pressure and inertial forces as the liquid imbibes. The hydrostatic pressure P_H of the liquid column can be described as:

$$P_H = h\rho g \quad (20)$$

where h is the height of the liquid column, ρ stands for liquid density and g for gravity acceleration. When the hydrostatic and the interfacial pressure differences are equated, the maximal height of the capillary rise h_{max} may be calculated:

$$h_{max} = \frac{2\gamma_L \cos\theta}{\Delta\rho g r} \quad (21)$$

Symbol $\Delta\rho$ stands for the density difference across the LV interface.

To express the viscous dissipation of liquid, the Hagen-Poiseuille's law is used which describes a moving liquid in a capillary. Assuming the laminar flow and no slip conditions the pressure difference across the capillary ΔP_η is expressed as:

$$\Delta P_\eta = \frac{8h\eta}{r^2}\frac{dh}{dt} \quad (22)$$

The symbol η means liquid dynamic viscosity and t represents time in which the liquid pass in h distance in capillary. Finally the relation for inertial forces is[15,17,44,46,47]:

$$P_i = \rho\left[h\frac{d^2h}{dt^2} + \left(\frac{dh}{dt}\right)^2\right] \quad (23)$$

The effect of inertial forces can be neglected since it is significant only in the early stage of penetration or when r is large or η very small[48]. As long as the wicking height is small, the hydrostatic pressure is also negligible, but after period of time the liquid column ceases to rise due to the balance of surface tension and gravity[46]. When omitting the inertia and gravitation the resulting balance can be reduced to:

$$\frac{2\gamma_L \cos\theta}{r} = \frac{8h\eta}{r^2}\frac{dh}{dt} \quad (24)$$

The integration with the initial conditions of h = 0 and t = 0 leads to the familiar equation which was independently developed by Lucas and Washburn equation[49,50]:

$$h^2 = \frac{\gamma_L r \cos\theta}{2\eta} t \quad (25)$$

This relates the height of capillary rise (or more precisely the distance of penetration) to the penetration time in a cylindrical capillary[15,17,44,46,47].

In the case of the penetration into a porous media the single capillary is substituted with a bundle of the cylindrical capillaries characterized by mean or effective pore radius into which the kinetics of the penetration is the same as for the real porous medium[15,17,44,46,47]. However, the model may be insufficient especially for the porous solids with wide distribution of the pore sizes. Moreover, the effective pore radius of a network of capillaries with varying radius determined by Lucas-Washburn equation may differentiate from the radius obtained by other measurements, such as mercury porosimetry or nitrogen adsorption[51].

Instead of the rate of capillary rise, the measurement of the capillary pressure change ΔP which accompanies the capillary rise of a liquid into a tube packed with powder can be performed using equation (19)[52].

Irregular pores

It is natural that real porous solids have mostly very complicated structures containing pores which are often denominated as cavities, channels, interstices etc. The pores can be distinguished according to the size on micropores, having widths smaller than 2 nm, mesopores, ranging from 2 to 50 nm, and macropores which achieve more than 50 nm diameter. The size of the pores is the major parameter for the porous solids characterization; therefore, number of methods for the pore size distribution analysis exists. As regards the types of pores, they can be closed, opened, blind or through and can be also classified according to the shapes into cylindrical, angular, ink-bottle, funnel or slit-shaped pores[53].

For estimation of the wetting properties in irregular pore structures, idealized systems have to be often used, such as cylinders, prisms, spheres or periodic surfaces, which preferably resemble the original pore structure because the capillarity in irregular pores may be quite anomalous.

For example angular pores undergo different filling stages and spontaneous displacement during the transition from dry to wet and vice versa. Under dry conditions the liquid first accumulates in the corners due to capillary forces and then the capillary radius of curvature increases until the liquid menisci contact each other (Figure 4). After that the middle part of the pore is filled. When the pore is drained, the liquid first leaves the central part and a fraction of the liquid remains in the corners, which is not possible in the cylindrical tubes. The Cassie-Baxter equation can be incorporated into the capillary rise model because it is possible to treat the angular pore with liquid filled corners as a round channel with composite surface consisting of solid and liquid surface[13,54].

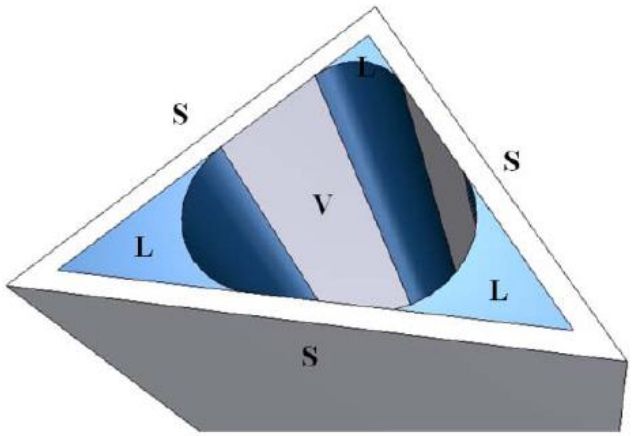

Figure 4 : Triangular pore with liquid filled corners

Further some computation approaches were developed allowing calculation of wicking distance versus time which use for example sinusoidal tube shape simplification to represent disturbances of broad and narrow passages in pores. A convenient approach is also to describe a pore as a sum of various segments of cosine functions[55].

Wetting properties of irregular porous solid depends also on its history of wetting and drying. A hysteresis in liquid retention may be observed which may stem from differences in advancing and receding CAs during filling and drainage of pores, air-entrapment in irregular pores, 'ink-bottle' effect resulting from the fact that the drainage of non-uniform pores is governed by the smaller pore radius, the changing radius of curvature of pores etc.[13].

CONTACT ANGLE MEASUREMENT OF DISCRETE SOLIDS

The measurement of the contact angle is necessary to estimate the wetting properties of solids. However, it should be mentioned that contact angle characterizes the whole wetting system with its interactions rather than the solid surface itself.

Several approaches have been proposed for CA measurement but only a few of them such as capillary penetration and thin layer wicking techniques were intended for being used on porous solids. Nevertheless, in some cases also other methods such as Wilhelmy method and sessile drop method have been used. Besides, it is also feasible to evaluate the CA from the heat of immersion measurement based on the calorimetric observation, which is beyond the scope of this paper and hence no more details will be discussed. Regardless the used method, it is essential to consider which CA can be obtained with respect to the principle of the measurement.

Washburn method

The most frequently used technique for powdered solids is probably Washburn method as the large amount of published research papers may indicate. The method is based on the Washburn equation (25), where the porous solid is treated as a bundle of cylindrical capillaries with mean or equivalent pore radius r*[5,17]:

$$h^2 = \frac{\gamma_L r^* \cos\theta}{2\eta} t \qquad (26)$$

Two main experimental procedures can be used: either the penetration distance or the liquid mass gain measurement. The relation between liquid mass m and height h in the column of porous material is given as follows:

$$m = \pi R_k^2 h \rho \varepsilon \qquad (27)$$

Letter R_k stands for the radius of the column, symbol ρ is liquid density and ε represents porosity of the material packed in the column. This can be substituted into eq. (26) to obtain modified Washburn equation, which allows the interpretation of the liquid mass gain vs. time measurement:

$$m^2 = \left[\frac{r^*(\pi R_k^2)^2 \varepsilon^2}{2}\right] \frac{\rho^2 \gamma \cos\theta}{\eta} t = C \frac{\rho^2 \gamma \cos\theta}{\eta} t \qquad (28)$$

Symbol C is the solid material constant comprising the term in the square brackets, which reflects the pore geometry of the solid[17].

Figure 5 shows an experimental set-up for the Washburn technique. The solid sample is suspended on a microbalance. The tested material can be fixed by means of solid sample holder or in the case of discrete solid it is packed into a glass tube with a frit at the bottom. The sample is brought into contact with the liquid surface in the vessel and the liquid rises into the pores due to the capillary action[56]. It is usually believed that the upper CA limit is 90° to allow the spontaneous liquid penetration. Nevertheless some authors report CA as high as 115°, which may be in some cases joined with small volume of liquid reservoir[11,12].

Review

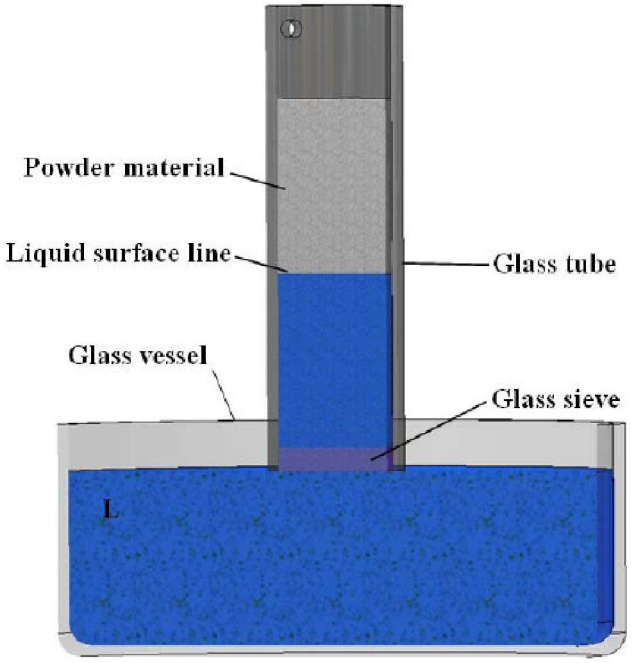

Figure 5 : Experimental set-up of the Washburn measuring technique using glass tube with packed powder material

When the mass of the wicking liquid is measured as a function of time, then two unknown remain: the contact angle θ and the constant C, as can be seen in the eq. (28). Hence, it is necessary to determine this constant in advance by performing the measurement with a liquid under the condition of perfect wetting (where θ = 0°), which is usually some alkane e.g. n-hexane, heptane, octane. The determined value of constant C is used in the subsequent measurement with another test liquid, which allows the calculation of the contact angle. Very common testing liquids are water, formamide, glycerol and ethylene glycol as polar and diiodomethane or α-bromonaphtalene as non-polar liquids[5,56].

Unfortunately, the indirect experiment may result in many inaccuracies. It is essential to use reproducible samples with the same size, weight and measure of compression in the case of powders. Also the assumption of the zero CA for the material constant evaluation may be erroneous[45,51,56]. There are also other questionable topics such as the influence of the wetting line velocity, adsorption of the liquid vapour on the solid sample or the irregular capillaries in the porous system[48,57]. It should be also mentioned that the Washburn technique gives rather advancing CA than receding or equilibrium one and the values of solid surface free energy (SSFE) calculated from this CA may be inaccurate[5,57-59].

Even through the mentioned problems, the capillary rise technique has been frequently used in whole range of materials such as natural fibres, wood, soil, stone, ceramics, fabrics, paper, pigment[7,9,10,14,17,56,58]. Moreover, some studies appeared to use this technique for estimation of the porosity[14,23,60].

Thin-layer wicking method

This technique is a modification of the Washburn method, therefore it arises from the same principle, as suggested by van Oss *et. al.*[61,62]. It is designed to measure contact angles of discrete solids and the main difference stems from the preparation of the sample.

A powdery sample can be deposited on a microscopic glass slide in the form of aqueous slurry and dried or the glass can be sprayed with glue and shaken in a flask with the sample. The glass covered with thin porous layer of the tested material is then suspended on a microbalance and after the slide touches the liquid surface, the liquid soaks up the slide through the capillaries formed between the particles deposited on the glass surface. The wicking experiment can be proceeded not only with these vertical and open-air samples but also the horizontal set-up and the sandwich chambers enclosing powdery materials are used. As well as in the Washburn method, the distance of penetration or the weight of the soaking liquid may be measured to obtain contact angle[18,57,59,62]. The method is not intended only for powders but also fibres can be used[62-65].

Wilhelmy method

The Wilhelmy method is based on balancing the forces of surface tension (ST), gravity and buoyancy acting on a sample with well defined shape suspended vertically in the LV interface. For a known length of wetted perimeter of the sample P, the force F acting on the balance can be represented as:

$$F = mg + P\gamma_L \cos\theta - V\rho g \quad (29)$$

Letter m stands for sample mass, V is the immersed volume of the sample, ρ is the liquid density and the rest is as usual. Extrapolating the trend of the total force to the zero depth of immersion where the buoyancy is zero and assuming the constant sample weight following equation is valid:

$$F = P\gamma_L \cos\theta \quad (30)$$

The wetted perimeter can be determined either by di-

rect size measuring or using a liquid of known ST for which the CA is supposed to be zero such as n-hexane[1,12,20]. Then the CA of the liquid formed on the solid surface can then be gained. The method inheres in the measurement of the force acting during immersion on the wetted perimeter of the sample via weight monitoring.

Figure 6 shows a scheme of an experimental set-up for the Wilhelmy technique. The sample with a constant perimeter is suspended on a thin rod from the electro-balance. The united porous solid such as fabrics can be fasten by means of solid sample holder while the measurement of the powders can be accomplished using a plate covered with a thin powder layer just like in the previous method. One end of the sample is then submerged into a liquid. Both, advancing and receding CAs can be obtained by immersing the plate into or withdrawing if from the liquid at constant speed[1,45,66]. It is essential to measure both CAs mainly in the case of heterogeneous surface where the advancing CA is mostly representative for low-energy surface portion whereas the receding CA is indicative of the higher-energy portion[12].

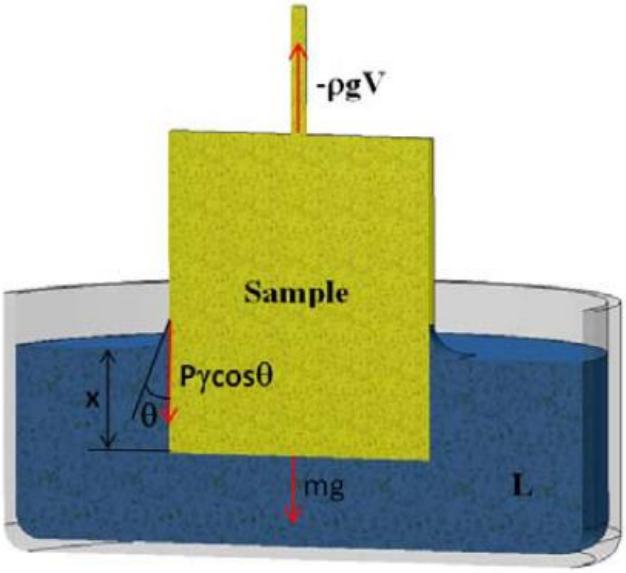

Figure 6 : Experimental set-up of Wilhelmy measurement method

Although the method was originally intended for using on flat compact surface, many researches introduce some corrections to adapt it on porous solids. One of the most common difficulties in experiments using porous samples is the absorption of the liquid. This can be reduced using liquids which yield CA higher than 90°. Further, whole range of modifications has been used such as: the immersion speed alternation; however, this can deform the L meniscus, end-sealing of the samples and Washburn-like mass correction to involve the absorbed L[12,20]. Another inaccuracy can spring from the wetted perimeter determination. The application of the effective perimeter instead of the geometrical one is indisputable but in the case of the glass slide with glue fixed powder layer it can be quite questionable whether to treat it as a composite surface. The method has been applied on whole range of porous stones, wood, non-woven fabrics, powder[12,20-22].

Methods based on shape of drop or bubble

Another valuable tool to obtain the CA of solids is the sessile drop method based directly on Young equation (7), where a liquid drop is placed on the horizontal solid surface. The drop volume can be increased or decreased in order to establish advancing and receding mode. Adhering gas bubble method is symmetrical only with the difference that a gas bubble is placed under the solid immersed in the liquid. The CA can be directly read using telescope with goniometric scale, which is not very accurate but immediately available. Another option is the CA evaluation from the photographic or digital images by a computer program using proper fitting strategy to the experimental drop profile, which is known as Axisymmetric Drop Shape Analysis (ADSA).

It is possible to evaluate the CA either from the drop profile or from the diameter (referred as ADSA-P or ADSA-D). In the former case the angle between the plane of SL interface and the tangent to the LV interface crossing in the three phase contact line is measured, as illustrated in figure 1. This way is more favourable for higher CA. In the letter the diameter of the drop is experimentally measured from the above view, which brings more advantages to low CA but also more input parameters are necessary in comparison to the profile approach. In any case the establishment of finite CA is crucial[1,8,45].

The approach was initially proposed for smooth flat surfaces and the application on the real and porous solids is accompanied with high CA variability mainly due to the lack of drop symmetry and the loss of volume by capillary action. Despite this problem the ad-

Review

aptation for non-ideal surfaces occurred. Some precautions should be followed e.g. the drop has to be symmetric and the volume sufficiently large with respect to roughness and heterogeneity proportion[8,29]. The time between deposition and image acquisition or CA reading should be kept to a minimum to avoid volume changes due to the evaporation and absorption. Regardless the type of surface, a drop should be every time placed on a new surface that had not been in contact with a liquid previously and when acquiring the images factors like illumination, focusing and relative placement of the camera to the drop should be considered[8].

The two mentioned techniques are commonly used for flat solids but have been already used also on porous stones, wood, cell layers *etc*.[8,12]. Notwithstanding the liquid absorption of drop by the porous material can be considered a problem, it can be turned to profit in some applications. For materials with high suction rate and capacity and hydrophobic materials with CA above 90° the Washburn experiment does not work. But optical CA measurement can provide proper results by the measuring of CA versus age of the droplet placed on the material, which is enabled mainly due to the availability of high-speed video equipment in recent years. Also the drop penetration time is measured which denotes time taken for the drop to penetrate completely into the porous substrate with no liquid remaining on the surface. This has already been successfully used on tissue materials used for diapers, cosmetic tissues, further writing and printing papers *etc*.[68-70].

ESTIMATION OF SOLID SURFACE FREE ENERGY

Although in some applications the estimation and comparison of the contact angles is sufficient, the CA data are mostly converted to solid surface free energy, which allows the characterization of the solid surface without having to explicitly describe the test liquids. Several different models were developed. The right choice depends on the nature of the tested solid (polar, non-polar, high- or low-energy material) and the required results (only total surface energy or dispersive and polar contributions etc.). The proper selection of the type and number of liquid results from the chosen model and it should also enable to characterize all types of the interactions contributing to the solid surface free energy (SSFE) to obtain reliable results.

Intermolecular interactions

The non-covalent and non-electrostatic intermolecular forces which are collectively called Lifshitz-van der Waals interactions (LW) can be divided into three groups according to the origin. First group defined by Keesom includes the interactions operating between two molecules (1 and 2) with permanent dipoles. The energy of interaction between such molecules is dependent on the thermal energy k_BT, as can be deduced from the following equation:

$$V_{12}^{Keesom} = -\frac{2\mu_1^2\mu_2^2}{3(4\pi\varepsilon_0)^2 k_B T r^6} = -\frac{C_{12}^P}{r^6} \quad (31)$$

The meaning of the symbols is as follows: V - the potential energy, μ_1 and μ_2- dipole moments of molecules 1 and 2, ε_0- dielectric permitivity, k_B - Boltzman constant, T - absolute temperature and r - the distance between the interacting molecules.

Second type of LW interactions is induced interaction between molecule with a permanent dipole and a neighboring neutral molecule referred as Debye interactions. The potential energy of these forces between different molecules may be given as:

$$V_{12}^{Debye} = -\frac{\alpha_1\mu_2^2 + \alpha_2\mu_1^2}{(4\pi\varepsilon_0)^2 r^6} = -\frac{C_{12}^I}{r^6} \quad (32)$$

Letter α denotes the polarizability of molecules. The potential energy is independent of the temperature because the induced dipole follows the motion of the permanent dipole apart from the thermal motion.

The last type of LW interactions, which are named after London, is generated as a consequence of random fluctuations in polarization of molecules. This leads to a creation of temporary dipoles influencing each other. Although these forces are the weakest compared to the previous types, they are the most significant because they appear in all kinds of molecules, not only those containing polar molecules. The so called dispersive interaction energy between unlike molecules may be described using the following formula:

$$V_{12}^{London} = -\frac{3\alpha_1\alpha_2}{2(4\pi\varepsilon_0)^2 r^6}\frac{I_1 I_2}{I_1 + I_2} = -\frac{C_{12}^L}{r^6} \quad (33)$$

$I = h\nu$ is the ionization energy where h stands for Planck constant and ν for the frequency of fluctuation.

The constants C_{12}^P, C_{12}^I, C_{12}^L which occur in the equations (31)-(33) characterize subsequently the polar, induced and London's interactions between molecules 1 and 2. These three types of interactions use to be included into one term because they are all inversely proportional to the sixth root of the distance between interacting molecules and the total LW interaction energy is then given by a sum of these components.

Other forces influencing the magnitude of surface chemistry are Lewis acid-base interactions which are generated between electron acceptor (acid) and electron donor (base). They appear in the compounds containing hydrogen bonds - strong secondary bonds between atoms of hydrogen and a highly electronegative element such as F, O, N and Cl or other compounds interacting with Lewis acids and bases[71,72].

Fowkes approach

Fowkes theory[71-78] represents a basis for surface energy estimation mainly for the calculation of dispersive components of the SSFE. Fowkes proposed that SFE is a measure of attractive forces between solid and liquid and that the contributions of the attractive forces are additive. Total SFE is therefore a sum of all energy components arising from various intermolecular interactions acting between the components of the same kind:

$$\gamma = \gamma^D + \gamma^K + \gamma^I + \gamma^H + \gamma^{AB} + \ldots \quad (34)$$

the superscript L expresses dispersive (London) interactions, K means Keesom interactions, I stands for Debye (induced) forces, H denotes hydrogen bonds and AB are interactions between acids and bases.

Practically, the total SFE is divided only in two parts: dispersive γ^D and non-dispersive γ^N fusing all non-dispersive components:

$$\gamma = \gamma^D + \gamma^N \quad (35)$$

Fowkes assumed that only the interactions functioning across the interface assist to the adhesion and thus only dispersive forces are important in this respect. The geometric mean approach was exerted for the interface energy calculation:

$$\gamma_{SL} = \gamma_S + \gamma_L - 2\sqrt{\gamma_S^D \gamma_L^D} \quad (36)$$

The symbols γ^D_S and γ^D_L mark dispersive parts of ST of solid and liquid. After joining the equations (7), (8) and (36) following formula can be obtained which was developed by Good[79] and Fowkes[52]:

$$W_A = \gamma_L(\cos\theta + 1) = 2\sqrt{\gamma_S^D \gamma_L^D} \quad (37)$$

This enables the calculation of dispersive portion of SSE γ^D_S from the experimentally acquired values of θ, γL and γ^D_L. If a non-polar liquid is used then $\gamma_L = \gamma^D_L$ and it is possible to write:

$$1 + \cos\theta = 2\sqrt{\gamma_S^D / \gamma_L} \quad (38)$$

It should be mentioned that the equations (36) and (37) are valid only the case when both the liquid and solid are non-polar but it is also possible to gain acceptable results when only one of them is non-polar.

OWRK approach

Owens, Wendt, Rabel and Kaelble[72,73,75,76,78,80] extended Fowkes theory also for the situations when both dispersive and polar interfacial forces act across the interface, which covers all cases when the solid and liquid are polar. It is assumed that dispersive parts of both phases interact with each other as well as the polar parts but there are no interactions between polar and dispersive forces. The SFE value is computed as a sum of dispersive and polar portions i.e. $\gamma = \gamma^D + \gamma^P$. The interfacial tension may be written as:

$$\gamma_{SL} = \gamma_S + \gamma_L - 2\sqrt{\gamma_S^D \gamma_L^D} - 2\sqrt{\gamma_S^P \gamma_L^P} \quad (39)$$

Introducing equations (7) and (8) into this relation leads to:

$$W_A = \gamma_L(\cos\theta + 1) = 2\sqrt{\gamma_S^D \gamma_L^D} + 2\sqrt{\gamma_S^P \gamma_L^P} \quad (40)$$

The measurement with two liquids with known γ^D_L and γ^P_L values (commonly water and methylene iodide) allows the estimation of the dispersive and polar parts of SSFE.

Practically, the results obtained by this approach are not absolutely confidential because various test liquids provide various polarity values of given solid. This springs from the fact that the term polar contribution covers all non-dispersive components which mostly include also asymmetric donor-acceptor interactions which can not be described with common geometric mean approach.

Dalal suggested a method for the parallel solution of several equations when more than two test liquid are used, which offers more reasonable results. It is based on the least square method and the formula in subsequent form:

Review

$$\frac{1+\cos\theta}{2}\frac{\gamma_L}{\sqrt{\gamma_L^D}} = \sqrt{\gamma_S^D} + \sqrt{\gamma_S^P}\sqrt{\frac{\gamma_L^P}{\gamma_L^D}} \quad (41)$$

which may be successfully applied particularly on polar systems.

Wu - harmonic mean approach

Also according to this approach[72,75] surface energy is equal to the sum of dispersive and polar parts γ^D and γ^P. The only difference is the harmonic mean method used for the calculation:

$$\gamma_{SL} = \gamma_S + \gamma_L - 4\left(\frac{\gamma_S^D\gamma_L^D}{\gamma_S^D+\gamma_L^D} + \frac{\gamma_S^P\gamma_L^P}{\gamma_S^P+\gamma_L^P}\right) \quad (42)$$

By substituting relations (5) and (8) into (42) a final formula for surface energy contribution can be derived:

$$(1+\cos\theta_i)\gamma_{Li} = 4\left(\frac{\gamma_S^D\gamma_{Li}^D}{\gamma_S^D+\gamma_{Li}^D} + \frac{\gamma_S^P\gamma_{Li}^P}{\gamma_S^P+\gamma_{Li}^P}\right) \quad (43)$$

The subscript Li indicates the use of several liquids. This procedure is convenient mainly for low-energy systems such as water and polymers.

The combination of geometric and harmonic mean method is also feasible:

$$(1+\cos\theta_i) = 2\sqrt{\gamma_S^D\gamma_{Li}^D} + 4\frac{\gamma_S^P\gamma_{Li}^P}{\gamma_S^P+\gamma_{Li}^P} \quad (44)$$

or

$$(1+\cos\theta_i) = 2\sqrt{\gamma_S^P\gamma_{Li}^P} + 4\frac{\gamma_S^D\gamma_{Li}^D}{\gamma_S^D+\gamma_{Li}^D} \quad (45)$$

These equations provide good results mainly in systems with high energies for instance glasses, oxides ands metals.

It should be remarked that utilization of the liquid with similar values of polar and dispersive parts leads to erroneous results of surface energy; hence, a parameter D for two different liquids denoted with i and j is introduced:

$$D = \sqrt{(\gamma_L^D)_i(\gamma_L^P)_j} - \sqrt{(\gamma_L^D)_j(\gamma_L^P)_i} \quad (46)$$

If the value of the parameter is equal or higher than 10mN/m (or 10 mJ/m^2) the liquid combination can be used for the measurement. Generally, the method is more suitable for measurement between polymers and commonly available liquids.

Equation of state approach

Another group of models[72,73,78,79,81-85] is based on the thermodynamic equation of state in the following form: $\gamma_{SL} = f(\gamma_L, \gamma_S)$ where the interfacial tension γ_{SL} depends only on the values of γ_S and γ_L.

Berthelot suggested following relation known as Berthelot's combining rule:

$$\gamma_{SL} = \gamma_L + \gamma_S - 2\sqrt{\gamma_L\gamma_S} \quad (47)$$

The incorporation of eq. (7) into this formula leads to:

$$\cos\theta = -1 + 2\sqrt{\frac{\gamma_S}{\gamma_L}} \quad (48)$$

This simplifies calculation of the γ_S and θ values and consequent re-substitution into Young equation enables the acquirement of γ_{SL} value.

Ward and Neumann stated a formula for low-energy surfaces:

$$\gamma_{SL} = \frac{(\sqrt{\gamma_S} - \sqrt{\gamma_L})^2}{(1 - 0{,}015\sqrt{\gamma_S\gamma_L})} \quad (49)$$

The introduction of the Young equation provides a way for γ_S calculation from the known values of contact angle:

$$\cos\theta = \frac{\gamma_L + (0{,}015\gamma_S - 2)\sqrt{\gamma_S\gamma_L}}{\gamma_L(0{,}015\sqrt{\gamma_S\gamma_L} - 1)} \quad (50)$$

Considering the deviations from the geometric mean, it is usual to introduce an empirical parameter which serves as a correlation factor. In this connection the coefficient is referred as interaction parameter Φ:

$$W_A = \gamma_S + \gamma_L - \gamma_{SL} = 2\Phi\sqrt{\gamma_S\gamma_L} \quad (51)$$

The interaction parameter equals to 1 for ideal phase boundaries. Good[79] attempt to calculate the interaction parameter Φ (which ranged from 0,53-1,17) by means of statistical thermodynamic but only for relatively simple systems which did not include hydrogen bonds and interactions conveying the charge transfer. Because the theoretical computation of the interaction parameter for more complex systems is too troublesome, an empirical relation was suggested by Neumann:

$$\Phi = e^{-\beta.(\gamma_L-\gamma_S)^2} \quad (52)$$

The term β is an universal constant [β = 0,0001247 (m^2/mJ)^2] which returns relatively good results on low energy surfaces but similarly to other one-liquid approaches the choice of liquid affects the resulting γ.

Li and Neumann combined eq. (47), (51) and (52) and derived following formula:

$$\gamma_{SL} = \gamma_L + \gamma_S - 2\sqrt{\gamma_L \gamma_S}.e^{-0,0001247.(\gamma_L - \gamma_S)^2} \quad (53)$$

Subsequent joining with Young equation yields:

$$\cos\theta = -1 + 2\sqrt{\frac{\gamma_S}{\gamma_L}}.e^{-0,0001247.(\gamma_L - \gamma_S)^2} \quad (54)$$

The next relation was outlined as the equation of state by Wu:

$$\gamma_C = \frac{\gamma_L (1+\cos\theta)^2}{4} \quad (55)$$

Here γ_C is a function of the interaction parameter and surface free energy. The value of γ_S is derived from the dependence $\gamma_C = f(\theta)$ as a maximal value $\gamma_{C\,max}$.

Acid – base approach

Van Oss, Good and Chaudhury[52,71-75,86-88] quite lately proposed this Lifshitz–van der Waals/ acid–base theory. According to this approach the SSFE equals to a sum of two components:

$$\gamma = \gamma^{LW} + \gamma^{AB} \quad (56)$$

Symbol γ^{LW} is a contribution of the Lifshitz-van der Waals (LW) forces including London, Keesom and Debye interactions because they show identical distance dependence and can be therefore treated with the same combining rule. Another part of surface energy γ^{AB} is joined with Lewis acid–base (AB) forces caused by electron transfer between donors and acceptors. One of the most ordinary interactions of this type is hydrogen bonding. The polar part of surface energy γ^{AB} can acquire positive or negative value and is separated in two non-additive parts: electron-acceptor (acidic) γ^+ and electron-donor (bacic) γ^-:

$$\gamma^{AB} = 2\sqrt{\gamma^+\gamma^-} \quad (57)$$

Surface energy can then be calculated as:

$$(1+\cos\theta)\gamma_L = 2(\sqrt{\gamma_L^{LW}\gamma_S^{LW}} + \sqrt{\gamma_L^+\gamma_S^-} + \sqrt{\gamma_L^-\gamma_S^+}) \quad (58)$$

The left hand side represents cohesion in the liquid and the right hand side adhesion between S and L. There are three unknowns (γ^{-LW}_S, γ^{-+}_S, γ^-_S) remaining in the relation and thus the measurement with three liquid is required. At least two should be polar and one of them is recommended to be water. If more than three liquids are used the least square method can be applied in the following form:

$$\frac{1+\cos\theta_i}{2}\frac{\gamma_{Li}}{\sqrt{\gamma_{Li}^{LW}}} = \sqrt{\gamma_S^{LW}} + \sqrt{\gamma_S^+}\sqrt{\frac{\gamma_{Li}^-}{\gamma_{Li}^{LW}}} + \sqrt{\gamma_S^-}\sqrt{\frac{\gamma_{Li}^+}{\gamma_{Li}^{LW}}} \quad (59)$$

The subscript Li designates i-th liquid and θ_i is contact angle measured with i-th liquid. In comparison with the three liquids calculation, the regression method is more resistant against ill-conditioning due to bad liquid choice. The result is usually very close to value obtained with recommended liquid set.

Zisman approach

Zisman[72,75,76,87] noticed that the correlation of cosθ and γ_L is very often linear. Zisman method is based on the measurement of the dependence of cosθ on total surface tension of liquids γ_L, which can be expressed as: $\cos\theta = f(\gamma_L)$.

After the linear extrapolation $\cos\theta \rightarrow 1$ is applied, the value of critical surface tension γ_C is acquired, which corresponds to the situation when the liquid ideally wets the solid surface i.e. $\theta = 0°$. The dependence can be described with a function:

$$\cos\theta = 1 + b.(\gamma_C - \gamma_L) \quad (60)$$

Parameter b is a constant typical for a series of used liquids. It should be emphasized that the procedure is valid only for obtaining γ^{LW}_S of solids with the apolar liquids. In addition, the value of γ_C characterizes the molecules on the solid surface but it does not correspond to total surface energy.

LIST OF SYMBOLS AND ABBREVIATIONS

A	: Area
α_1, α_2	: polarizability of molecules 1 and 2
AB	: acid - base
ACCA	: actual contact angle
APCA	: apparent contact angle
β	: universal constant [β = 0,0001247 (m^2 $mJ^{-1})^2$]
C	: Washburn material constant
$C_{12}^{P\,(I,\,L)}$	: constants characterizing polar (induced, london) interactions
D	: parameter in eq. (46)
ε, ε_0	: porosity, dielectric permitivity
f (f1, f2, fi)	: fraction of wetted area (containing component 1, 2 or i)
F	: Helmholtz free energy, force

Review

Φ : interaction parameter
g : gravity acceleration
G : Gibbs free energy
γ : surface tension
γ_C : critical surface tension
γ_{Cmax} : maximal value of the function $\gamma_C=f(\theta)$ from eq. (55)
γ_{LV} ($=\gamma_L$) : liquid-vapour interfacial tension = liquid surface tension
γ_{SL} : solid-liquid interfacial tension
γ_{SV} ($=\gamma_S$) : solid-vapour interfacial tension = solid surface tension (energy)
γ_S^0 : γ_S of the solid surface in equilibrium with its own vapour
γ_S^D (γ_L^D) : dispersive parts of surface tension
θ_S : static contact angle
θ_W : Wenzel contact angle
θ_Y : Young (ideal) contact angle
P : wetted perimeter
ΔP : pressure difference
P_H : hydrostatic pressure
P_i : pressure caused by inertial forces
$\Delta P\eta$: pressure caused by viscous forces
r : capillary radius, roughness factor, distance between molecules
r* : equivalent pore radius
r_f : roughness ratio of the wet area of rough composite surface
R : radius of the SL contact circle of liquid drop on a solid in the plane of the solid
R_1, R_2, R : radii of the curvature of an interface
R_k : radius of the column (tube)
$\gamma^{D\,(K, I, H, AB, N)}$: energy contributions due to dispersive (Keesom, induced, hydrogen bonding, acid-base and non-dispersive) interactions
γ_L^{AB} (γ_S^{AB}) : acid-base part of γ_L (γ_S)
γ_L^{LW} (γ_S^{LW}) : Lifshitz-van der Waals – dispersive part of γ_L (γ_S)
γ_S^P (γ_L^P) : polar parts of surface tension (energy) or solid (liquid)
$\gamma+$, $\gamma-$: electron-acceptor (electron-donor) part of surface energy
h : high of capillary rise, hysteresis, Planck constant
η : dynamic viscosity
I_1, I_2 : ionization energy
k_B : Boltzman constant ($k_B = 1{,}380658.10^{-23}$ $J.K^{-1}$)
l : length
L : liquid phase
LW : Lifshitz - van der Waals
μ_1, μ_2 : dipole moments of molecules 1 and 2
n : molar amount
P : pressure
π_e : film pressure
θ : contact angle
θ_A : advancing contact angle
θ_C : Cassie contact angle
θ_{CB} : Cassie-Baxter contact angle
θ_D : dynamic contact angle
θ_{MS} : most stable contact angle
θ_R : receding advancing contact angle
ρ : density
S : solid phase, spreading coefficient
SSE (SSFE) : solid surface energy (solid surface free energy)
t : time
T : temperature
V : volume, vapour phase
V_{12}^{Keesom} : potential energy caused by Keesom interactions
V_{12}^{Debye} : potential energy caused by Debye interactions
V_{12}^{London} : potential energy caused by London interactions
W : work
W_A (W_{12}) : work of adhesion (between different molecules 1 and 2)
W_C (W_{11}) : work of cohesion (between the same molecules of the phase 1)
W_{LL} (W_{SS}) : work of cohesion in a liquid (solid)
x : distance

ACKNOWLEDGEMENT

This article was created with support of Operational Program Research and Development for Innovations co-funded by the European Regional Development Fund (ERDF) and national budget of Czech Republic within the framework of the Centre of Polymer Systems project (reg. number CZ. 1.05 / 2.1.00 / 03. 0111).

REFERENCES

[1] C.N.C.Lam, J.J.Lu, A.W.Neumann; In Handbook of Applied Surface and Colloid Chemistry, Krister Holmberg, (Ed.); John Wiley & Sons: England, **14**, 251-277 **(2002)**.

[2] S.M.Kumar, A.P.Deshpande; Colloids Surf.A, **277**, 157 **(2006)**.

[3] X.D.Wang, X.F.Peng, D.J.Lee; Description of Dynamic Contact Angle on a Rough Solid Surface, Proceedings of the ASME Summer Heat Transfer Conference, Las Vegas, Nevada, USA, July 21-23, **(2003)**.

[4] E.Chibowski, R.Perea-Carpio; J.Colloid Interface Sci., **240**, 473 **(2001)**.

[5] I.Yildrim; Thesis, Virginia Tech., **(2001)**.

[6] A.Siebold, M.Nardin, J.Schultz, A.Walliser, M.Oppliger; Colloids Surf.A, **161**, 81 **(2000)**.

[7] Z.Peršin, K.Stana-Kleinschek, T.Kreže; CCACAA, **75**, 271 **(2002)**.

[8] M.A.Rodríguez-Valverde, M.A.Cabrerizo-Vílchez, P.Rosales-López, A.Páez-Dueñas, R.Hidalgo-Álvarez; Colloids Surf.A, **206**, 485 **(2002)**.

[9] J.Gassan, V.S.Gutowski, A.K.Bledzki; Mater.Eng., **283**, 132 **(2000)**.

[10] M.E.P.Wålinder, D.J.Gardner; In 'Apparent and Microscopic Contact Angles', J.Drelich, J.S.Laskowski, K.L.Mittal, (Ed); VSP: The Netherlands, 419-430 **(2000)**.

[11] K.Grundke; In 'Handbook of Applied Surface and Colloid Chemistry', K.Holmberg, (Ed); John Wiley & Sons: England, **2**, 119-142 **(2002)**.

[12] C.Della Volpe, A.Penati, R.Peruzzi, S.Siboni, L.Toniolo, C.Colombo; In 'Apparent and Microscopic Contact Angles', J.Drelich, J.S.Laskowski, K.L.Mittal, (Ed); VSP: The Netherlands, 349-375 **(2000)**.

[13] D.Or, M.Tuller; In 'Encyclopedia of Soils in the Environment', 1st Edition, D.Hiller, (Ed); Elsevier: U.K, **1**, 155-163 **(2005)**.

[14] E.P.Kalogianni, T.Savopoulos, T.D.Karapantsios, S.N.Raphaelides; Colloids Surf.B, **35**, 159 **(2004)**.

[15] A.Hamraoui, T.J.Nylander; Colloid Interface Sci., **250**, 415 **(2002)**.

[16] F.M.Etzler; In 'Contact Angle, Wettability and Adhesion', K.L.Mittal, (Ed); VSP: The Netherlands, **3**, 219-264 **(2003)**.

[17] T.Dang-Vu, J.Hupka; Physicochemical Problems of Mineral Processing, **39**, 47 **(2005)**.

[18] E.Chibowski, F.González-Caballero; Langmuir, **9**, 330 **(1993)**.

[19] L.Holysz, E.Chibowski; Langmuir, **8**, 717 **(1991)**.

[20] M.Brugnara, C.Della Volpe, D.Maniglio, S.Siboni, M.Negri, N.Gaeti; In 'Contact Angle, Wettability and Adhesion', K.L.Mittal, (Ed); VSP: The Netherlands, **4**, 115-141 **(2006)**.

[21] X.Pepin, S.Blanchon, G.Couarraze; Int.J.Pharm., **152**, 1 **(1997)**.

[22] X.Pepin, S.Blanchon, G.Couarraze; Powder Technol., **99**, 264 **(1998)**.

[23] Z.Li, R.F.Giese, C.J.Van Oss, H.M.Leech, H.E.Burdette; J.Am.Ceram.Soc., **77**, 2220 **(1994)**.

[24] I.Tyomkin; In ,'Contact Agle, Wettability and Adhesion', 1st Edition, K.L.Mittal, (Ed); VSP: The Netherlands, **2**, 165-176 **(2002)**.

[25] D.E.Packham; 'Handbook of Adhesion', 2nd Edition, John Wiley & Sons: England, **(2005)**.

[26] E.M.Petrie; Omnexus, Adhesives & Sealants: Interphase and Interface, http://www.omnexus4 adhesives.com/adhesiveknowledge/editorials. aspx?id=33; September 10, **(2007)**.

[27] E.M.Petrie; Omnexus, Adhesives & Sealants: Substrate Surface Dynamics, http://www.omnexus 4adhesives.com/ gettingstarted /editorials.aspx?id=35; September 10, **(2007)**.

[28] P.Reynolds; In 'Colloid Science: Principles, Methods and Applications', 1st Edition, T.Cosgrove, (Ed); Blackwell Publishing: UK, 159-179 **(2005)**.

[29] A.Marmur; Soft Matter, **2**, 12 **(2006)**.

[30] P.C.Hiemenz; In 'Principles of Colloid and Surface Chemistry', 2nd Revised and Expanded Edition, MARCEL DEKKER: New York, 287-345 **(1986)**.

[31] A.W.Adamson, A.P.Gast; In 'Physical Chemistry of Surfaces', 6th Edition, John Wiley & Sons: USA, 347-382 **(1997)**.

[32] R.J.Hunter; In 'An Introduction to Modern Colloid Science' [s.l.], Oxford University Press, 131-163 **(1999)**.

[33] G.Wolanski, A.Marmur; Langmuir, **14**, 5292 **(1998)**.

[34] P.S.Swain, R.Lipowski; Langmuir, **14**, 6772 **(1998)**.

[35] R.N.Wenzel; Ind.Eng.Chem., **28**, 988 **(1936)**.

[36] C.Ishimo, K.Okumura, D.Queré; Europhys.Lett., **68**, 419 **(2004)**.

[37] A.Marmur; Langmuir, **19**, 8343 **(2003)**.

[38] A.B.D.Cassie; Discuss.Faraday Soc., **3**, 11 **(1948)**.

[39] J.Drelich, J.D.Miller; Langmuir, **9**, 619 **(1993)**.

[40] A.B.D.Cassie, S.Barter; Trans.Faraday Soc., **40**, 546 **(1944)**.

[41] Y.Pomeau, E.Villermaux; Today, **59**, 39 **(2006)**.

[42] R.Fürstner, W.Barthlott; Langmuir, **21**, 956 **(2005)**.

Review

[43] P.G.De Gennes; Reviews of Modern Physics, **57**, 827 **(1985)**.
[44] G.Martic, J.De Coninck, T.D.Blake; J.Colloid Interface Sci., **236**, 213 **(2003)**.
[45] A.W.Adamson, A.P.Gast; In Physical Chemistry of Surfaces, 6th Edition, John Wiley & Sons: USA, 4-43 **(1997)**.
[46] W.Zhong, X.Ding, Z.L.Tang; Textile Research Journal, **71**, 762 **(2001)**.
[47] M.Lago, M.Araujo; Physica A, **289**, 1 **(2001)**.
[48] G.Martic, F.Gentner, D.Seveno, D.Coulon, J.De Coninck, T.D.Blake; Langmuir, **18**, 7971 **(2002)**.
[49] R.Lucas; Kolloid Z., **23**, 15 **(1918)**.
[50] E.W.Washburn; Phys.Rev., **17**, 273 **(1921)**.
[51] A.Marmur, R.D.Cohen; J.Colloid Interface Sci., **189**, 299 **(1997)**.
[52] C.J.Van Oss; Colloids Surf.A, **78**, 1 **(1993)**.
[53] J.Rouquerol, D.Avnir, C.W.Fairbridge, D.H.Everett, J.H.Haynes, N.Pernicone, J.D.Ramsay, K.S.W.Sing, K.K.Unger; Pure & Appl.Chem., **66**, 1739 **(1994)**.
[54] F.Kemling; Thesis, Lulea University of Technology, **(2003)**.
[55] T.L.Staples, D.G.Shaffer; Colloids Surf.A, **204**, 239 **(2002)**.
[56] C.Rulison; Krüss Technical Note #302: Wettability Studies for Porous Solids Including Powders and Fibrous Materials, **(1996)**.
[57] E.Chibowski, R.Perea-Carpio; Adv.Colloid Interface Sci., **98**, 245 **(2002)**.
[58] M.Brugnara, E.Degasperi, C.Della Volpe, D.Maniglio, A.Penati, S.Siboni; In 'Contact Angle, Wettability and Adhesion', K.L.Mittal, (Ed); VSP: The Netherlands, **4**, 143-164 **(2006)**.
[59] K.Grundke, A.Augsburg; J.Adhes.Sci.Technol., **14**, 765 **(2000)**.
[60] C.Rulison; Krüss Technical Note #236e: The Washburn "C" Factor for Characterization of Porous Coatings, **(2003)**.
[61] C.J.Van Oss, R.F.Giese, Z.Li, K.Murphy, J.Norris, M.K.Chaudhury, R.J.Good; J.Adhes.Sci.Technol., **6**, 413 **(1992)**.
[62] W.Wu, R.F.Giese Jr., C.J.Van Oss; Powder Technol., **89**, 129 **(1996)**.
[63] L.Hołysz; J.Mater.Sci., **35**, 6081 **(2000)**.
[64] B.Simončič, L.Černe, B.Tomšič, B.Orel; Cellulose, **15**, 47 **(2008)**.
[65] F.Dourado, M.Mota, H.Pala, F.M.Gama; Cellulose, **6**, 265 **(1999)**.
[66] G.S.Lapham, D.R.Bowling, W.W.Schultz; Exp.Fluids, **27**, 157 **(1999)**.
[67] C.Della Volpe, D.Maniglio, M.Morra, S.Siboni; Colloids Surf.A, **20**, 47 **(2002)**.
[68] J.U.Zilles; Krüss Technical Note # 221e: Wettabilities and Surface Tensions of Different Paper Types, **(2000)**.
[69] U.T.Reinhard; Krüss Technical Note #222e: How Absorbent are Diapers? **(2000)**.
[70] K.P.Hapgood, J.D.Litster, S.R.Biggs, T.Howes; J.Colloid.Interface Sci., **253**, 353 **(2002)**.
[71] C.J.Van Oss, M.K.Chaudhury, R.J.Good; Chem. Rev., **88**, 927 **(1988)**.
[72] V.Buršíková, P.Sťahel, Z.Navrátil, J.Buršík, J.Janča; Surface Energy Evaluation of Plasma Treated Materials by Contact Angle Measurement, V.Buršíková, P.Sťahel, Z.Navrátil, (Ed); Masaryk University: Brno, **(2004)**.
[73] D.Y.Kwok, A.W.Neumann; Adv.Colloid Interf.Sci., **81**, 167 **(1999)**.
[74] D.Y.Kwok, D.Li, A.W.Neumann; Langmuir, **10**, 1323 **(1994)**.
[75] Contact Angle Measurement: A Theoretical Approach, www.kruss.info; November 9, **(2007)**.
[76] F.K.Hansen; The Measurement of Surface Energy of Polymer by Means of Contact Angles of Liquids on Solid Surfaces: A Short Overview of Frequently Used Methods, http://folk.uio.no/fhansen/surface_energy.pdf; November 10, **(2007)**.
[77] F.M.Fowkes; Ind.Eng.Chem., **56**, 40 **(1964)**.
[78] N.T.Correia, J.J.Moura Ramos, B.J.V.Saramago, J.C.G.Balado; J.Colloid Interface Sci., **189**, 361 **(1997)**.
[79] L.A.Girifalco, R.J.Good; J.Phys.Chem., **61**, 904 **(1957)**.
[80] D.K.Owens, R.C.Wendt; J.App.Polymer Sci., **13**, 1741 **(1969)**.
[81] D.Y.Kwok, A.W.Neumann; Colloids Surf.A, **161**, 31 **(2000)**.
[82] D.Y.Kwok, A.W.Neumann; Colloids Surf.A, **161**, 49 **(2000)**.
[83] R.E.Johnson Jr., R.H.Dettre; Langmuir, **5**, 293 **(1989)**.
[84] R.J.Good; **(1977)**.
[85] D.Li, A.W.Neumann; Adv.Colloid Interface Sci., **39**, 299 **(1992)**.
[86] C.J.Van Oss, R.J.Good, M.K.Chaudhury; Langmuir, **4**, 884 **(1988)**.
[87] E.M.Petrie; In 'Handbook of Adhesives and Sealants', McGraw-Hill: USA, 49-90 **(2000)**.
[88] D.Y.Kwok; Colloids Surf.A, **156**, 191 **(1999)**.